Pergamon

Int. J. Heat Mass Transfer. Vol. 39, No. 7, pp. 1453–1462, 1996

0017-9310/96 $15.00 + 0.00

0017-9310(95)00235-9

Turbulent buoyant thermal in a density-stratified atmosphere

G. M. MAKHVILADZE and J. P. ROBERTS
University of Central Lancashire, Department of Built Environment, Preston PR1 2HE, U.K.

and

S. E. YAKUSH
Institute for Problem in Mechanics, Russian Academy of Sciences, Ave. Vernadskogo, 101, Moscow, 117526, Russia

(*Received* 23 *May* 1994 *and in final form* 21 *March* 1995)

Abstract—A model of a turbulent axisymmetric thermal rising in an atmosphere with altitude-dependent density is proposed. A numerical study of the thermal is performed for an isothermal atmosphere with exponentially decreasing density. The structure of the thermal corresponding to the square-root law of the ascent is obtained in similarity coordinates. An analytical solution is found for a wide class of the density variation functions and studied in detail for an inverse-square law of density diminution with height. It is shown that as the thermal penetrates the low-density atmospheric layers, its top edge becomes less sharp and the width of the thermal increases. However, the self-similar coordinate of the cloud top remains almost constant and the square-root law of the ascent still holds.

1. INTRODUCTION

The free convective flows accompanying the evolution of a hot buoyant cloud (thermal) in a stratified ambience have attracted much attention over the past few decades. Previous experimental and theoretical studies have shown that when a thermal is ascending in an incompressible neutrally stratified medium, after some period the fluid motion becomes self-similar after which the vertical coordinate of the cloud top increases with time according to a 'square-root' law, i.e. proportionally to $t^{1/2}$ (e.g. [1, 2]). The self-similar stage begins after the thermal 'forgets' the initial conditions so that the characteristic length scale no longer exists in the flowfield.

Many earlier studies of the thermals dealt with relatively simple models in which the volume-averaged characteristics of the buoyant clouds were under consideration and the shape of the cloud was assumed to be spherical or toroidal (e.g. [1–3]). Such models enable only the gross (integral) parameters of the thermal (i.e. its height, diameter, mean temperature and concentration, velocity of the ascent) to be predicted.

A more detailed description of the internal structure of an ascending thermal was obtained by solving the incompressible fluid dynamics equations using the Boussinesq approximation to determine spatial distributions of velocity, temperature and concentration in the buoyant cloud. The analytical solutions were obtained for low values of the Rayleigh number in refs. [4–6]. A theory of atmospheric turbulent thermals at high Rayleigh numbers was offered in ref. [7] and developed further in refs. [8, 9] where the equations of an incompressible fluid were solved using a vertical boundary layer assumption. Numerical and analytical solutions describing the internal structure of a self-similar thermal in the incompressible atmosphere were offered e.g. in refs. [7–11]. Only the temperature stratification of the atmosphere was taken into account in these works while the atmospheric density was considered to be constant.

The assumption of constant ambient density is valid if the compressibility of the medium is small. This is normally the case for convection in liquids as well as for a 'weak' atmospheric convection when the vertical scale of the convective flow is much less than the characteristic vertical scale at which the density varies significantly with height. Conversely, if the thermal is powerful enough it can penetrate high atmospheric layers reaching elevations of about 8–10 km. At such altitudes the effects of compressibility of the air become substantial and the density diminishes noticeably in comparison with its value near the ground. Strictly speaking, in this case the flowfield is not self-similar, because the length scale associated with vertical density distribution still exists even after the initial conditions are 'forgotten'. Yet, the experimental data on dynamics of large-scale thermals gives a clear evidence that the square-root law still holds in this case [12].

Though some analytical and numerical calculations of the large-scale thermals resulting from powerful

NOMENCLATURE

a	auxiliary function in temperature profile (20)
C_P	specific heat of the gas at constant pressure
g	acceleration due to gravity
H	length scale of vertical distribution of the atmospheric density
J	stratification parameter
L	length scale
p	pressure deviation
P	pressure
Q	total heat energy
Q_0	initial heat release
R	gas constant
r	radial coordinate
r_0	initial radius of the thermal
T	temperature
t	time
t_D	characteristic time relevant to the effects of the density stratification
t_I	initial stage duration
t_J	characteristic time relevant to the effects of the temperature stratification
U	velocity scale
u	radial velocity
v	vertical velocity
z	vertical coordinate.

Greek symbols

α	coefficient of isothermal compressibility
$B(p, q)$	beta function
$B_x(p, q)$	incomplete beta function
B_0	total initial buoyancy of the thermal
β	coefficient of thermal expansion
γ	ratio of specific heats, $C_P/(C_P-R)$
ε	constant in asymptotic function $\hat{\xi}$
ζ	transformed non-dimensional coordinate
ζ_*	point of intersection of the zero isoclines ξ_1, ξ_2
Θ	temperature scale
θ	temperature deviation, $T-T_a$
Λ	auxiliary function in the analytical solution (23)
Λ_0	integration constant in analytical solution
λ	heat conductivity
μ	dynamic viscosity
ξ	vertical velocity and temperature profile in the analytical solution
ξ_1, ξ_2	zero isoclines of the differential equation (21)
ρ	density
Σ_1, Σ_2	auxiliary integrals
τ	non-dimensional time, $(t/t_D)^{1/2}$
Φ	auxiliary function in the analytical solution (23)
φ	non-dimensional atmospheric density
Ψ	stream function
Ω	vorticity.

Non-dimensional complexes

Gr	Grashof number
Pr	Prandtl number.

Subscripts

0	value at the level of the virtual source
a	undisturbed atmosphere
D	value relative to density stratification
I	value relative to the initial stage
J	value relative to temperature stratification
m	value at the maximum point
t	top edge of the cloud

Superscripts

0	initial value
^	approximation of ξ by the partially linear function for calculation of the integral Σ_2
~	similarity variable.

near-ground explosions have been reported recently [13–16], a detailed theoretical description of the thermal in a variable-density atmosphere has yet to be developed. A numerical and analytical study of the structure of the thermal ascending in a medium with variable density is the scope of the current paper.

2. STATEMENT OF THE PROBLEM

We consider the evolution of an axisymmetric thermal formed in the atmosphere as a result of an instantaneous release of a certain amount of heat Q_0. We suppose that in the undisturbed atmosphere the temperature T_a varies with height, the pressure P_a and the density ρ_a distributions satisfy the hydrostatic equilibrium condition and the equation of state. We also assume that the heat release occurred in a small region whose dimensions are much smaller than the characteristic height at which the atmospheric density changes significantly. This means that the ambient density can be considered constant during the initial period of the buoyant cloud evolution until it reaches the similarity stage. We introduce the virtual source as an apparent origin of the rising cloud and use the parameters of the atmosphere at this point as reference values.

The evolution of the axisymmetrical thermal is described in the cylindrical coordinate system (r, z)

originated at the virtual source, z axis being directed vertically upward and r axis being directed radially. We suppose that the deviations of the temperature θ and pressure p are small compared to the values of T_a and P_a, respectively. If so, the gas density ρ can be substituted by the atmospheric density ρ_a except in the term describing the buoyancy force in the vertical momentum equation. This term is proportional to the difference between the atmospheric and local density and can be related to the pressure and temperature deviations by linearising the equation of state

$$\rho(P, T) \approx \rho_a(P_a, T_a)[1 + \alpha p - \beta\theta], \quad \text{where} \quad \alpha = P_a^{-1} \quad \beta = T_a^{-1}. \tag{1}$$

We consider here only the slow (subsonic) convection, hence below we neglect the dynamic compressibility effects in comparison with thermal expansion, i.e. we assume that $|\alpha p| \ll |\beta\theta| \ll 1$. Since, normally, the temperature varies with height more slowly than the density, we neglect also the variation of the thermal expansion coefficient β with height and assume that $\beta = T_0^{-1}$.

The main difference of this approach from the 'classic' Boussinesq approximation (see e.g. [2]) is that the linearization in equation (1) is performed relative to the local values of the undisturbed density, $\rho_a(z)$, rather than relative to some particular (fixed) value of the density. This enables the atmospheric density variation with height caused by the weight compressibility of the gas to be taken into account.

Within the limits and assumptions made above, the problem can be reduced to the solution of the following system of equations

$$\frac{\rho_a}{r}\frac{\partial ur}{\partial r} + \frac{\partial \rho_a v}{\partial z} = 0 \tag{2}$$

$$\frac{\partial \rho_a u}{\partial t} + \frac{\rho_a}{r}\frac{\partial u^2 r}{\partial r} + \frac{\partial \rho_a uv}{\partial z} = -\frac{\partial p}{\partial r} + \mu\left(\frac{1}{r}\frac{\partial}{\partial r}r\frac{\partial u}{\partial r} + \frac{\partial^2 u}{\partial z^2}\right) \tag{3}$$

$$\frac{\partial \rho_a v}{\partial t} + \frac{\rho_a}{r}\frac{\partial uvr}{\partial r} + \frac{\partial \rho_a v^2}{\partial z} = -\frac{\partial p}{\partial z} + \mu\left(\frac{1}{r}\frac{\partial}{\partial r}r\frac{\partial v}{\partial r} + \frac{\partial^2 v}{\partial z^2}\right) + \rho_a g\beta\theta \tag{4}$$

$$\frac{\partial \rho_a \theta}{\partial t} + \frac{\rho_a}{r}\frac{\partial u\theta r}{\partial r} + \frac{\partial \rho_a \theta v}{\partial z} = \frac{\lambda}{C_P}\left(\frac{1}{r}\frac{\partial}{\partial r}r\frac{\partial \theta}{\partial r} + \frac{\partial^2 \theta}{\partial z^2}\right) - \frac{\rho_a v J}{g\beta} \tag{5}$$

$$J = g\beta\left(\frac{dT_a}{dz} + \frac{g}{C_P}\right) = -g\left(\frac{d\ln\rho_a}{dz} + \frac{g}{\gamma RT_a}\right), \tag{6}$$

where J is the stratification parameter proportional to the difference between the local temperature gradient and the dry adiabatic gradient $-g/C_P$; the second expression in the right-hand side of equation (6) is obtained by using the ideal gas equation of state. It can be seen that for a given stratification parameter J, the vertical density distribution in the atmosphere is characterized by the length scale $H = RT_0/g$ so that

$$\rho_a(z) = \rho_0 \varphi\left(\frac{z}{H}\right), \tag{7}$$

where ρ_0 is the density of the atmosphere at the virtual source level.

The symmetry boundary condition is posed at the axis for each variable ($u = 0$, $\partial v/\partial r = \partial\theta/\partial r = 0$), while the absence of disturbances is assumed at infinity ($u = v = \theta = 0$).

Turbulent coefficients of the dynamic viscosity μ and conductivity λ are assumed constant. This turbulence model, though relatively simplistic, enables the observed square-root law of ascent of the thermal to be obtained in the calculations, not only in the case of the incompressible atmosphere (e.g. [8–11]), but also for a thermal rising in a variable-density environment [13–15]. Also, for constant turbulent transport coefficients, an analytical solution can be found, which is always an important reason for justifying the simplifications made. Bearing in mind the analytical as well as numerical solution of the problem, we used the model which was of the minimum complexity and, at the same time provided the dynamics of the thermal consistent with that observed experimentally [12].

3. GOVERNING PARAMETERS

We consider the evolution of the thermal after release of the heat Q_0. To perform the dimensional analysis it is convenient to introduce the total initial buoyancy of the thermal B_0 defined as

$$B_0 = \frac{g\beta Q_0}{2\pi\rho_0 C_P}. \tag{8}$$

The Grashof and Prandtl numbers are expressed as

$$Gr = \frac{B_0}{(\mu/\rho_0)^2} \quad Pr = \frac{\mu C_P}{\lambda}.$$

We note that the Grashof and Prandtl numbers are based here on the turbulent, rather than laminar, transport coefficients. The experimentally measured turbulent Prandtl number for well-developed turbulent air flows is of the order and slightly less than 1, a recent review concerned with this can be found in ref. [17].

Consider now the time scales relevant to different stages of the evolution of the thermal. At the initial stage a vortex ring flowfield is being formed and the buoyant cloud converts into a shape-preserving convective element. The duration of the initial stage t_I was obtained in numerical calculations in ref. [18] for uniform initial distribution of the temperature over the bulk of the hot cloud and in ref. [13] for Gaussian initial temperature distribution. The average duration

of the initial stage of the evolution turned out to be about $t_I \approx (3 \div 4) r_0^2/B_0^{1/2}$ where r_0 is the initial radius of the thermal. At $t \gg t_I$ the solution no longer depends on the initial distributions and the coordinate of the cloud top edge increases with time according to the square-root law $z_t \sim t^{1/2}$.

The effects of the temperature stratification of the atmosphere become substantial after a period of about $t_J = |J|^{-1/2}$. After this moment the square-root law of ascent no longer holds: if $J > 0$ (stably stratified atmosphere) the thermal decelerates and stabilizes at some altitude, otherwise (unstable stratification) it accelerates.

If the thermal rises high enough, after some time t_D it reaches the elevation at which the ambient density ρ_a differs substantially from that at the level of the virtual source ρ_0. This means that for $t > t_D$ the density variation with height becomes essential and the atmosphere can no longer be regarded as uniform. The characteristic time t_D can be introduced as a period over which the top edge of the buoyant cloud travels the distance equal to the characteristic vertical scale of the atmospheric density variation H (see equation (7)). For the thermal in an incompressible atmosphere it was shown in refs. [7–9] that during the self-similar stage the coordinate of the cloud top edge increases with time as

$$z_t = Gr^{1/4} B_0^{1/4} t^{1/2}. \tag{9}$$

Hence, density variation with height becomes significant after a period of

$$t_D = \frac{H^2}{(Gr \cdot B_0)^{1/2}} = \frac{H^2 \mu}{B_0 \rho_0}. \tag{10}$$

Of the three time scales discussed, the time t_J depends only on the atmospheric conditions while the scales t_I and t_D are determined by parameters of the thermal. Depending on the energy yield, initial size of the thermal and atmospheric conditions, various relationships between the time scales are possible, but normally $t_I \ll t_J, t_D$. If the total buoyancy of the cloud is relatively small, so that $t_D \gg t_J$, a density variation with height does not reveal itself during the square-root ascent of the self-similar thermal. This particular case corresponds to the applicability of the Boussinesq approximation. In other words, the solutions obtained earlier for an incompressible atmosphere (e.g. refs. [6–11]) correspond to the intermediate asymptotics $t_I \ll t \leqslant t_J \ll t_D$.

The current study is focused on another intermediate asymptotics $t_I \ll t$, $t_D \ll t_J$ which means that we still consider the time interval over which the atmospheric temperature stratification effects are negligible, and hence the last term in equation (5) can be omitted. Integration of equation (5) over the whole space, with allowance for the stated above boundary conditions, shows that the conservation of the total heat energy of the thermal

$$Q = 2\pi \int_{-\infty}^{\infty} \int_{0}^{\infty} \rho C_P \theta r \, dr \, dz = \text{const} = Q_0 \tag{11}$$

holds in this case. We expect that over the period $t_I \ll t \ll t_J$ the solution will coincide with that obtained for incompressible atmosphere, but as t becomes comparable to or greater than t_J, the density stratification effects will be manifested.

To analyse the structure of the thermal at the square-root stage of the ascent, we introduce the following length L, velocity U and temperature Θ scales

$$L = B_0^{1/4} t^{1/2} \quad U = Lt^{-1} \quad \Theta = \frac{U^2}{g\beta t^2} = \frac{B_0^{1/4}}{g\beta} t^{-3/2}. \tag{12}$$

This choice of the scales practically coincides with that employed in ref. [9] and slightly differs from analogous formulas used in ref. [11].

The main features of the evolution of the thermal in a variable-density medium were studied numerically for an atmosphere with exponentially decreasing density (which is the case for an isothermal environment), after that an analytical model was developed and used to investigate the thermal for the inverse-square decrease of the atmospheric density with height. The results are presented below.

4. NUMERICAL SOLUTION FOR EXPONENTIAL ISOTHERMAL ATMOSPHERE

We consider the ascent of a turbulent thermal in an isothermal ($T_a = \text{const} = T_0$) atmosphere. In this case the density distribution is exponential with characteristic height scale $H = RT_0/g$, so that $\varphi(z) = \exp(-z/H)$. To eliminate the pressure terms in the momentum equation we introduce the vorticity $\Omega = \partial u/\partial z - \partial v/\partial r$ and take the curl of the momentum equation. Also, we introduce the stream function Ψ so that

$$\frac{\partial \Psi}{\partial r} = \varphi v r \quad -\frac{\partial \Psi}{\partial z} = \varphi u r.$$

We introduce the new variables (denoted by tilde) using the scales defined in the equation (12): $\tilde{r} = r/L$, $\tilde{z} = z/L$, $\tilde{u} = u/U$, $\tilde{v} = v/U$, $\tilde{\theta} = \theta/\Theta$, $\tilde{\Psi} = \Psi/UL^2$, $\tilde{\Omega} = \Omega L/U$. The non-dimensional time is introduced as $\tau = (t/t_D)^{1/2}$, the vertical density distribution transforms then to $\varphi = \exp(-\tau Gr^{-1/4}\tilde{z})$. The problem reduces finally to solution of the following system of equations:

$$\frac{\partial^2 \tilde{\Psi}}{\partial \tilde{r}^2} - \frac{1}{\tilde{r}} \frac{\partial \tilde{\Psi}}{\partial \tilde{r}} + \varphi \frac{\partial}{\partial \tilde{z}} \varphi^{-1} \frac{\partial \tilde{\Psi}}{\partial \tilde{z}} + \varphi \tilde{r} \tilde{\Omega} = 0$$

$$\tilde{u} = -\frac{1}{\varphi \tilde{r}} \frac{\partial \tilde{\Psi}}{\partial \tilde{z}} \quad \tilde{v} = \frac{1}{\varphi \tilde{r}} \frac{\partial \tilde{\Psi}}{\partial \tilde{r}} \tag{13}$$

$$\frac{\tau}{2}\frac{\partial\varphi\tilde{\Omega}}{\partial\tau}+\frac{\partial}{\partial\tilde{r}}\left\{\varphi\tilde{\Omega}\left(\tilde{u}-\frac{\tilde{r}}{2}\right)\right\}+\frac{\partial}{\partial\tilde{z}}\left\{\varphi\tilde{\Omega}\left(\tilde{v}-\frac{\tilde{z}}{2}\right)\right\}+\varphi\frac{\partial\tilde{\theta}}{\partial\tilde{r}}$$

$$=Gr^{-1/2}\left\{\frac{1}{\tilde{r}}\frac{\partial}{\partial\tilde{r}}\tilde{r}\frac{\partial\tilde{\Omega}}{\partial\tilde{r}}-\frac{\tilde{\Omega}}{\tilde{r}^2}+\frac{\partial^2\tilde{\Omega}}{\partial\tilde{z}^2}\right\}$$

$$-\frac{\tau\varphi}{2}Gr^{-1/4}\left\{\tau\frac{\partial\tilde{u}}{\partial\tau}-\frac{\partial\tilde{u}\tilde{r}}{\partial\tilde{r}}-\tilde{z}\frac{\partial\tilde{u}}{\partial\tilde{z}}-\frac{\partial(\tilde{u}^2+\tilde{v}^2)}{\partial\tilde{r}}\right\} \qquad (14)$$

$$\frac{\tau}{2}\frac{\partial\varphi\tilde{\theta}}{\partial\tau}+\frac{1}{\tilde{r}}\frac{\partial}{\partial\tilde{r}}\left\{\varphi\tilde{\theta}\tilde{r}\left(\tilde{u}-\frac{\tilde{r}}{2}\right)\right\}+\frac{\partial}{\partial\tilde{z}}\left\{\varphi\tilde{\theta}\left(\tilde{v}-\frac{\tilde{z}}{2}\right)\right\}$$

$$=Gr^{-1/2}Pr^{-1}\left\{\frac{1}{\tilde{r}}\frac{\partial}{\partial\tilde{r}}\tilde{r}\frac{\partial\tilde{\theta}}{\partial\tilde{r}}+\frac{\partial^2\tilde{\theta}}{\partial\tilde{z}^2}\right\}. \qquad (15)$$

The boundary conditions on the axis of symmetry are $\tilde{\Psi}=\tilde{\Omega}=\partial\tilde{\theta}/\partial\tilde{r}=0$, at infinity $\tilde{\Psi}=\tilde{\Omega}=\tilde{\theta}=0$. The integral condition of constant heat energy in the thermal (equation (11)) takes the form

$$\int_{-\infty}^{\infty}\int_{0}^{\infty}\tilde{\theta}\tilde{r}\,\mathrm{d}\tilde{r}\,\mathrm{d}\tilde{z}=1. \qquad (16)$$

Initial distributions at $\tau=0$ correspond to the self-similar thermal rising in the incompressible (uniform-density) atmosphere. The set of equations (13)–(16) was solved numerically in a rectangular region $0\leqslant\tilde{r}\leqslant 4$, $-2\leqslant\tilde{z}\leqslant 7$ on a grid with 50×100 nodes, the marching along the τ variable was performed with step $\Delta\tau=0.05$. The distributions of all dependent variables at each time step were found by an iterative technique based on the line successive overrelaxation method [19].

To check the influence of the boundaries the results were compared with those obtained in larger regions $0\leqslant\tilde{r}\leqslant 6$, $-3\leqslant\tilde{z}\leqslant 9$ and $0\leqslant\tilde{r}\leqslant 8$, $-4\leqslant\tilde{z}\leqslant 14$ but with the same number of grid points. Though the increase in size of the domain led to a change in the position of the outermost streamlines, the structure and position of the thermal itself varied only slightly. The difference in the self-similar coordinates of the top edge of the cloud was 1% for the medium region and 2% for the largest region. The maximum values of the excess temperature differed by 2% for the medium region and 2.6% for the largest region, whilst the differences in the maximum values of the stream function were 2.5 and 5%, respectively. This implies that the size of the computational domain was large enough to eliminate the influence of the boundaries on the structure of the thermal.

We present now the results obtained for $Gr=400$, $Pr=1$. It is shown below that for this value of the turbulent Grashof number the self-similar coordinate of the cloud top edge coincides with the experimental data [12].

In Fig. 1 the structure of the thermal is presented in the similarity coordinates at $\tau=0$. It corresponds to the self-similar thermal in the incompressible atmosphere. The contours of the non-dimensional excess temperature $\tilde{\theta}$ are shown by solid lines for the temperature levels of 0.1, 0.2, ..., 0.9 of the maximum temperature $\tilde{\theta}_m=4.62$. The stream function contours are presented by dashed lines, the maximum value of the stream function is $\tilde{\Psi}_m=0.36$, the contours are also drawn with equal step (i.e. at 0.1, 0.2, ..., 0.9 of the maximum value $\tilde{\Psi}_m$). In the right side of Fig. 1 the vertical distribution of the ambient density $\varphi(\tilde{z})$ is also shown (note that only a part of the computational domain is shown, the upper and bottom boundaries of the computational domain extend beyond the picture). The similarity coordinate of the cloud top (defined as a height at which the excess temperature at the axis is equal to 0.1 of its maximum value $\tilde{\theta}_m$) is $\tilde{z}_t=4.26$, which is close to the experimental value (4.3 ÷ 4.4) found in ref. [12].

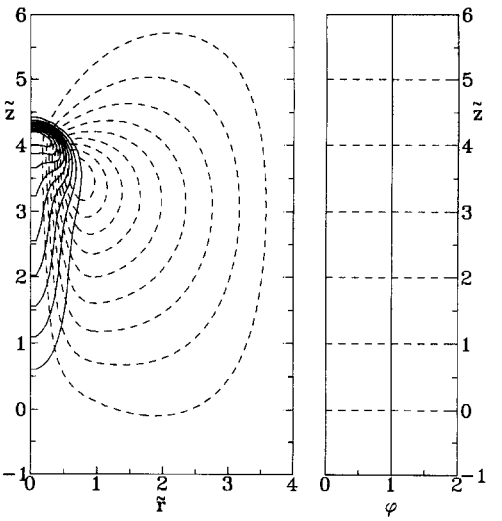

Fig. 1. Structure of the thermal in the similarity coordinates at $\tau=0$. Solid lines—contours of the temperature deviation $\tilde{\theta}$ (0.1, ..., 0.9 of the maximum value $\tilde{\theta}_m=4.62$), dashed lines—stream function $\tilde{\Psi}$ (0.1, ..., 0.9 of the maximum value $\tilde{\Psi}_m=0.36$). Atmospheric density distribution $\varphi(\tilde{z})$ is presented on the right.

As the time τ increases, the thermal advances into more and more rarefied layers of the atmosphere. The structure of the buoyant cloud at $\tau=1$ is shown in Fig. 2 ($\tilde{\theta}_m=4.82$, $\tilde{\Psi}_m=0.30$, $\tilde{z}_t=4.34$) together with the vertical distribution of the ambient density $\varphi(\tilde{z})$. In Fig. 3 the same distributions are presented at $\tau=2$ ($\tilde{\theta}_m=4.59$, $\tilde{\Psi}_m=0.26$, $\tilde{z}_t=4.53$). At this moment the density at the level of the cloud top edge is about 10 times less than at the virtual source level (the distance which the thermal passes over this period is about $2.5H$).

It can be seen from Figs. 1–3 that the structure of the buoyant cloud experiences some changes with time; the relative width of the thermal increases while the top edge of the cloud becomes less sharp. But the important thing is that cloud position in the similarity coordinates (namely, the vertical coordinate of its top edge) remains practically invariant. To demonstrate this, we present in Fig. 4 the time histories of the cloud top edge similarity coordinate $\tilde{z}_t$ and of the maximum

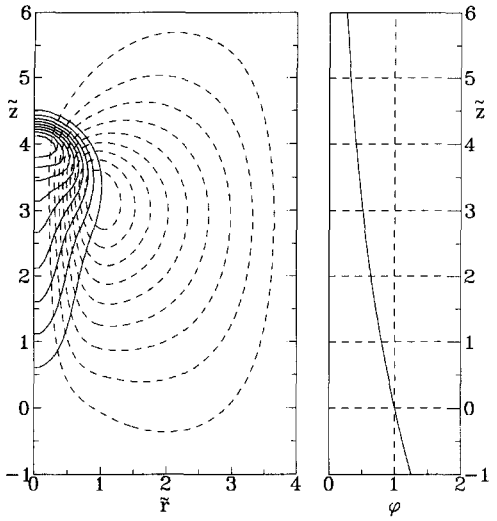

Fig. 2. Structure of the thermal at $\tau = 1$. Solid lines—contours of the temperature deviation ($\tilde{\theta}_m = 4.82$), dashed lines—stream function ($\tilde{\Psi}_m = 0.30$). On the right the vertical distribution of the atmospheric density $\varphi(\tilde{z})$ is presented.

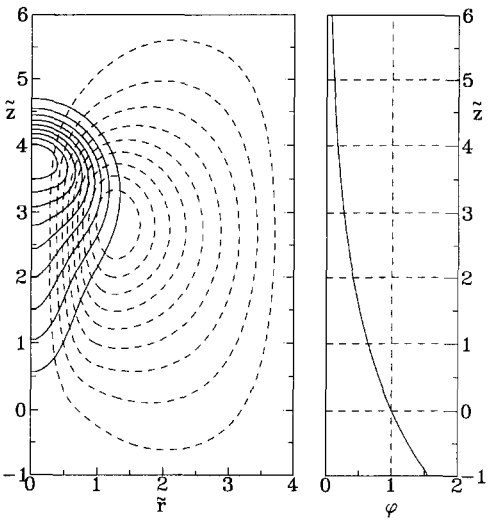

Fig. 3. Structure of the thermal at $\tau = 2$. Solid lines—contours of the temperature deviation ($\tilde{\theta}_m = 4.59$), dashed lines—stream function ($\tilde{\Psi}_m = 0.26$). On the right the vertical distribution of the atmospheric density $\varphi(\tilde{z})$ is presented.

excess temperature $\tilde{\theta}_m$ (curves 1 and 2, respectively), related to their initial values at $\tau = 0$ ($\tilde{z}_t^0 = 4.26$, $\tilde{\theta}_m^0 = 4.62$). The dashed curve denotes the density of the atmosphere at the level of the cloud top $\varphi(\tilde{z}_t)$. We can conclude that as the density drops about an order of magnitude, the position and parameters of the cloud remain almost invariant. This means that in physical coordinates the thermal rises according to the square-root law $z_t \sim t^{1/2}$ and the maximum excess temperature drops with time as $t^{-3/2}$.

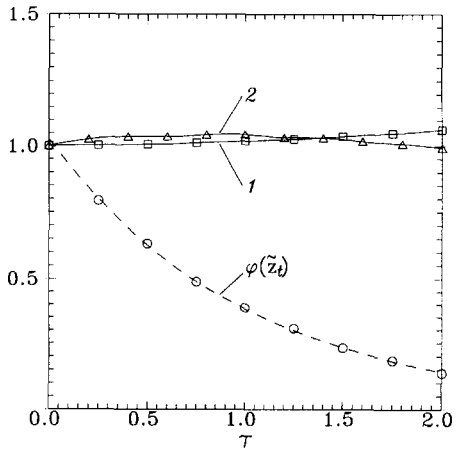

Fig. 4. Variation of the cloud top edge similarity coordinate $\tilde{z}_t$ (curve 1) and of the maximum excess temperature $\tilde{\theta}_m$ (curve 2) with non-dimensional time τ. Both functions are related to their initial values at $\tau = 0$ ($\tilde{z}_t^0 = 4.26, \tilde{\theta}_m^0 = 4.62$). Dashed line presents the atmospheric density at the level of the top edge $\varphi(\tilde{z}_t)$ as a function of time τ.

5. ANALYTICAL SOLUTION

For large Grashof numbers and $Pr = 1$ it is possible to find an analytic solution describing the thermal rising in the variable-density medium. Following refs. [7–9] we use the vertical boundary layer approximation and omit the pressure gradient term in the equation for the vertical momentum (4). It enables us to solve only the equations of continuity, vertical momentum and excess temperature. As before, we perform the substitution of variables as in equation (12) and consider the flowfield in similarity coordinates. The above results of the numerical modelling show that the structure of the thermal in similarity coordinates changes with time quite slowly, so we omit the temporal derivatives and seek for a solution which depends on τ only parametrically. After these simplifications have been made, the governing equations take the form

$$\frac{\partial \varphi \tilde{u} \tilde{r}}{\partial \tilde{r}} + \frac{\partial \varphi \tilde{v} \tilde{r}}{\partial \tilde{z}} = 0 \tag{17}$$

$$\varphi\left\{\frac{\tilde{v}}{2} + \left(\frac{\tilde{r}}{2} - \tilde{u}\right)\frac{\partial \tilde{v}}{\partial \tilde{r}} + \left(\frac{\tilde{z}}{2} - \tilde{v}\right)\frac{\partial \tilde{v}}{\partial \tilde{z}} + \tilde{\theta}\right\} + Gr^{-1/2}\left\{\frac{1}{\tilde{r}}\frac{\partial}{\partial \tilde{r}}\tilde{r}\frac{\partial \tilde{v}}{\partial \tilde{r}} + \frac{\partial^2 \tilde{v}}{\partial \tilde{z}^2}\right\} = 0 \tag{18}$$

$$\varphi\left\{\frac{3\tilde{\theta}}{2} + \left(\frac{\tilde{r}}{2} - \tilde{u}\right)\frac{\partial \tilde{\theta}}{\partial \tilde{r}} + \left(\frac{\tilde{z}}{2} - \tilde{v}\right)\frac{\partial \tilde{\theta}}{\partial \tilde{z}}\right\} + Gr^{-1/2}Pr^{-1}\left\{\frac{1}{\tilde{r}}\frac{\partial}{\partial \tilde{r}}\tilde{r}\frac{\partial \tilde{\theta}}{\partial \tilde{r}} + \frac{\partial^2 \tilde{\theta}}{\partial \tilde{z}^2}\right\} = 0. \tag{19}$$

We seek the solution of equations (17)–(19), assuming that the profiles of the vertical velocity $\tilde{v}$ and of the excess temperature $\tilde{\theta}$ are similar and described by the function

$$\tilde{v} = \tilde{\theta} = \frac{Gr^{1/4}}{2} \exp(-a(\tilde{z})\tilde{r}^2)\xi(\tilde{z}), \tag{20}$$

where, unlike refs. [7–9], some yet unknown function of the vertical coordinate $a(\tilde{z})$ is introduced into the argument of the exponent. Substitution of the profiles (20) into equations (18) and (19) shows that the similarity is possible for $Pr = 1$ only, this value is used in the following.

Integration of equation (20) gives the stream function

$$\tilde{\Psi} = \frac{\varphi}{4a} Gr^{1/4}(1 - \exp(-a\tilde{r}^2))\xi$$

after which the horizontal velocity $\tilde{u}$ can be found by differentiating the stream function as $\tilde{u} = -(\tilde{r}\varphi)^{-1} \partial\tilde{\Psi}/\partial\tilde{z}$. Upon substitution of the profiles (20) both equations (18) and (19) reduce to a single equation for the $\xi(\tilde{z})$ function (the prime denotes the differentiating with respect to $\tilde{z}$)

$$Gr^{-1/2}(\xi \exp(-a\tilde{r}^2))'' + \tfrac{1}{2}(\varphi\tilde{z}\xi \exp(-a\tilde{r}^2))'$$

$$= \exp(-a\tilde{r}^2)\left\{\frac{Gr^{1/4}}{4}\varphi(\xi^2)' + (4Gr^{-1/2}a - \varphi)(1 - a\tilde{r}^2)\xi + \frac{Gr^{1/4}}{2}a\xi^2(1 - \exp(-a\tilde{r}^2))\left(\frac{\varphi}{a}\right)'\right\}.$$

It can be seen that if we choose the yet unknown function in the horizontal profiles of the vertical velocity and of the excess temperature equation (20) as $a(\tilde{z}) = Gr^{1/2}\varphi(\tilde{z})/4$ the second and the third terms in the curly brackets become zero, that is why this function is used hereafter. We then average the remaining coefficients of the above equation by multiplying each of them by $\tilde{r}\,d\tilde{r}$ and integrating in the range from zero to infinity. Also, we introduce a new independent variable $\zeta = Gr^{-1/4}\tilde{z}$. As a result we obtain the following approximate ordinary differential equation for the function ξ (prime here denotes the differentiating with respect to ζ)

$$\frac{4}{Gr}\left(\frac{\xi}{\varphi}\right)'' + (2\zeta\xi - \xi^2)' = 0, \tag{21}$$

where the argument of the function φ vertical density distribution transforms from the physical coordinate z to the form $\varphi(z/H) = \varphi(\zeta\tau)$.

The integral condition (11) (or its analogue equation (16)) reduces then to the form

$$\int_{-\infty}^{\infty} \xi \, d\zeta = 1. \tag{22}$$

A general solution to equation (21), satisfying the boundary conditions $\xi = 0$ at $\zeta = \pm\infty$, is

$$\xi(\zeta) = \frac{4}{Gr} \frac{\exp(-\Phi(\zeta))}{\Lambda_0 + \Lambda(\zeta)}, \tag{23}$$

where

$$\Phi(\zeta) = \int_0^{\zeta} \left(\frac{Gr}{2}\zeta\varphi - \frac{\varphi'}{\varphi}\right) d\zeta$$

$$\Lambda(\zeta) = \int_{\zeta}^{\infty} \varphi \exp(-\Phi(\zeta)) \, d\zeta. \tag{24}$$

The integration constant Λ_0 in equation (23) depends on two parameters—Grashof number Gr and non-dimensional time τ. The value of Λ_0 can be obtained by substituting the solution (23) into the integral condition (22).

To analyse the solution (23) at arbitrary atmospheric density distribution $\varphi(\zeta\tau)$, we integrate it once with boundary conditions $\xi = 0$ at $\zeta = \pm\infty$ and obtain

$$\xi' = \frac{Gr}{4}\varphi\xi\left(\xi - 2\zeta - \frac{4}{Gr}(\varphi^{-1})'\right). \tag{25}$$

The zero isoclines of this equation are $\xi_1 = 0$ and $\xi_2 = 2\zeta + 4Gr^{-1}(\varphi^{-1})'$, we denote the point of their intersection as ζ_*. We suppose here that the function $\xi(\zeta)$ has a single maximum point $\zeta = \zeta_m$ where the vertical velocity v and the excess temperature $\tilde{\theta}$ assume their maximum values. A sufficient condition for the uniqueness of the maximum point is that for $\zeta < \zeta_*$ the isocline ξ_2 passes below ξ_1 (i.e. $2\zeta + 4Gr^{-1}(\varphi^{-1})' < 0$) while for $\zeta > \zeta_*$ the function ξ_2 increases monotonically (i.e. $2 + 4Gr^{-1}(\varphi^{-1})'' > 0$). We note that these conditions are satisfied for a wide range of functions φ and in particular for the exponential density distribution used above.

The point of maximum ζ_m can be found from the condition that the function $\xi(\zeta)$ intersects the zero isocline ξ_2, which means that the expression in the brackets in equation (25) turns to zero. Taking into account the definition of the function Φ from equation (24), we can recast the maximum condition to the form $\varphi\xi = 4Gr^{-1}\Phi'$, or finally

$$\varphi \exp(-\Phi) = \Phi'(\Lambda_0 + \Lambda). \tag{26}$$

We expand the function $\Lambda(\zeta)$ into an asymptotic series using the integration by parts

$$\Lambda(\zeta) = \int_{\zeta}^{\infty} \varphi \exp(-\Phi) \, d\zeta$$

$$= \frac{\exp(-\Phi)}{\Phi'}\left\{\varphi + \left(\frac{\varphi}{\Phi'}\right)' + 0\left(\frac{1}{(\Phi')^4}\right)\right\}.$$

Judging from the analytical solution found in refs. [7–9] for the uniform-density atmosphere as well as from the results of the numerical modelling presented above, we expect that the maximum is reached at $\zeta_m = 0(1)$, near the maximum point $\Phi' = Gr \cdot 0(1)$ and for large Grashof numbers we retain only the first two terms of the series omitting the terms of the order of

Gr^{-4} and less. As a result we obtain the maximum condition

$$\exp(-\Phi) = -\Lambda_0 \frac{\Phi'}{\left(\frac{\varphi}{\Phi'}\right)'}$$

$$= \Lambda_0 \left(\frac{Gr}{4}\right)^2 \frac{\varphi\left(2\zeta + \frac{4}{Gr}(\varphi^{-1})'\right)^3}{2 + \frac{4}{Gr}(\varphi^{-1})''}. \quad (27)$$

6. THERMAL IN THE ATMOSPHERE WITH INVERSE-SQUARE DENSITY DECREASE

The integration equation (22) necessary to calculate the constant Λ_0 in equation (23) can be performed analytically only in the simplest case when the density of the atmosphere is uniform ($\varphi = 1$), a corresponding solution was offered and studied in detail in refs. [7–9]. It has been shown that the function ξ increases with height, reaching its maximum at a point with coordinate (in our notation)

$$\zeta_m^0 \approx 1 - Gr^{-1} \ln\left(\frac{\pi Gr^3}{4}\right) \quad (28)$$

after which it decreases sharply, so that the function ξ can be approximated by a partially continuous function $\xi = 2\zeta$ for $0 \leqslant \zeta \leqslant 1$, $\xi = 0$ for $\zeta < 0$ and $\zeta > 1$.

For arbitrary density distribution φ it is impossible to calculate the integral equation (22) and to obtain explicit relationships describing the thermal. Below a particular case of the density distribution is studied in which approximate final formulas can be derived. Namely, the inverse-square diminution of the atmospheric density with height is considered

$$\varphi = \frac{1}{1 + (\tau\zeta)^2}. \quad (29)$$

This function satisfies the conditions considered above under which the vertical profile $\xi(\zeta)$ has a single maximum. This distribution can be regarded as a model describing at $\zeta \geqslant 0$ the density decrease with height.

Consider first the solution to equation (21) obtained numerically. In the right part of Fig. 5 the integral curves are presented at $\tau = 0.0, 1.0, 2.0, 3.0, 4.0$, in the left part corresponding atmospheric density distributions $\varphi(\zeta)$ are presented. It should be noted that the solution at $\tau = 0$ relates to the thermal rising in a uniform-density atmosphere. An analysis of Fig. 5 shows that as the thermal penetrates the rarefied atmospheric layers, the similarity coordinate of its top remains almost invariant (curves corresponding to different τ intersect at the same point). The point of maximum of the function $\xi(\zeta)$ slightly displaces downwards with time, while the horizontal size of the thermal increases proportional to $\varphi(\zeta_m)^{-1/2}$ and the

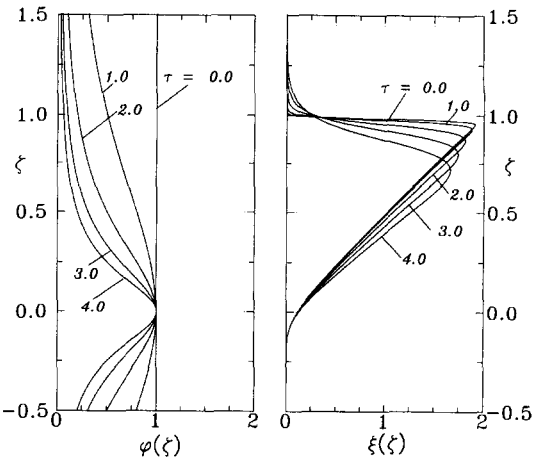

Fig. 5. Variation of the structure of the thermal rising in the atmosphere with density distributed with height according to the inverse-square law. The profiles presented correspond to the moments $\tau = 0.0, 1.0, 2.0, 3.0, 4.0$. In the left part the density distributions at the same moments are shown.

radius of the thermal in the similarity coordinates increases with time. These results are in a good agreement with those obtained in numerical integration of the complete set of equations performed above.

Consider now the results which can be obtained analytically. After substituting the density distribution (29) into equation (24) we explicitly obtain the auxiliary functions Φ and Λ

$$\Phi(\zeta) = \left(1 + \frac{Gr}{4\tau^2}\right) \ln(1 + (\zeta\tau)^2)$$

$$\Lambda(\zeta) = \int_\zeta^\infty \frac{d\zeta}{(1 + (\zeta\tau)^2)^{2 + \frac{Gr}{4\tau^2}}} =$$

$$\begin{cases} \frac{1}{2\tau} B_{\varphi(\zeta)}\left(\frac{1}{2}, \frac{3}{2} + \frac{Gr}{4\tau^2}\right) & \zeta \geqslant 0 \\ \frac{1}{\tau} B\left(\frac{1}{2}, \frac{3}{2} + \frac{Gr}{4\tau^2}\right) - \frac{1}{2\tau} B_{\varphi(\zeta)}\left(\frac{1}{2}, \frac{3}{2} + \frac{Gr}{4\tau^2}\right) & \zeta < 0, \end{cases}$$

where B is the beta function and B_x is the incomplete beta function [20, 21] the argument of which is the value of the function $\varphi(\zeta) = 1/(1 + (\zeta\tau)^2)$.

To find the constant Λ_0 we represent the integral in equation (22) as a sum of two terms Σ_1 and Σ_2

$$\int_{-\infty}^{\infty} \xi(\zeta)\, d\zeta = \int_{-\infty}^{\infty} \varphi\xi\, d\zeta + \int_{-\infty}^{\infty} (1 - \varphi)\xi\, d\zeta = \Sigma_1 + \Sigma_2.$$

The first of the two auxiliary integrals can be calculated exactly and expressed in terms of the beta function B

$$\Sigma_1 = \frac{4}{Gr}\ln\left(1+\frac{\Lambda(-\infty)}{\Lambda_0}\right)$$

$$= \frac{4}{Gr}\ln\left(1+\frac{1}{\Lambda_0\tau}\mathrm{B}\left(\frac{1}{2},\frac{3}{2}+\frac{Gr}{4\tau^2}\right)\right).$$

To calculate the integral Σ_2 we replace the function ξ in the integrand by an approximating function $\hat{\xi}(\zeta)$. We seek the asymptotics of the solution $\xi(\zeta)$ at $\zeta < \zeta_m$ using the pilot function $\xi(\zeta) = 2\zeta(1+\varepsilon\tau^2)$, where ε is an unknown as yet constant. Substitution of this function into equation (25) shows that its left and right-hand sides are equal asymptotically if $\varepsilon = 6/Gr$. We approximate the function $\xi(\zeta)$ by a discontinuous partially linear function

$$\hat{\xi}(\zeta) = \begin{cases} 2\zeta(1+\varepsilon\tau^2) & 0 \leqslant \zeta \leqslant \hat{\zeta}_m \\ 0 & \zeta < 0 \quad \zeta > \hat{\zeta}_m, \end{cases} \qquad (30)$$

where the coordinate of the maximum point $\hat{\zeta}_m = (1+\varepsilon\tau^2)^{-1/2}$ is determined from the integral relationship (22). The second auxiliary integral Σ_2 is then equal to

$$\Sigma_2 \approx \int_0^{\hat{\zeta}_m} \frac{(\tau\zeta)^2}{1+(\tau\zeta)^2}\hat{\xi}(\zeta)\,\mathrm{d}\zeta$$

$$= 1 - \frac{(1+\varepsilon\tau^2)}{\tau^2}\ln\left(1+\frac{\tau^2}{(1+\varepsilon\tau^2)}\right).$$

Substitution of the above values for Σ_1 and Σ_2 into the integral condition (22) gives the following result for the constant Λ_0

$$\Lambda_0 \approx \mathrm{B}\left(\frac{1}{2},\frac{3}{2}+\frac{Gr}{4\tau^2}\right)\tau^{-1}(1+\tau^2)^{-\left(\frac{3}{2}+\frac{Gr}{4\tau^2}\right)}.$$

We then substitute this value of Λ_0 into the maximum condition (27) to find the coordinate of the maximum point ζ_m. It is convenient to present the maximum point as $\zeta_m = \zeta_m^0 - \Delta\zeta_m$ where ζ_m^0 is the coordinate of the maximum point at $\tau = 0$ (i.e. in the case of a uniform-density atmosphere, see (28)) and $\Delta\zeta_m$ is its variation with time τ. Calculations give the following dependence

$$\Delta\zeta_m = \frac{\tau^2}{Gr}\ln\frac{\pi Gr^3}{4} - \frac{3}{Gr}(1+\tau^2)\ln(1+\tau^2). \qquad (31)$$

The function $\Delta\zeta_m(\tau)$ is presented in Fig. 6 by a solid curve together with the points obtained from numerical solution of equation (21). It can be seen that the approximate analytical solution gives the accuracy of prediction of the maximum point coordinate not worse than 25–30%. Even better accuracy can be achieved if when approximating the function $\xi(\zeta)$ in equation (30) we choose an appropriate slope of the linear function, i.e. the value of ε. The best fit was obtained for $\varepsilon \approx 8.8/Gr$, the corresponding dependence of the maximum point coordinate

$$\Delta\zeta_m = \frac{\tau^2}{Gr}\ln\frac{\pi Gr^3}{4} - \frac{4.4}{Gr}(1+\tau^2)\ln(1+\tau^2) \qquad (32)$$

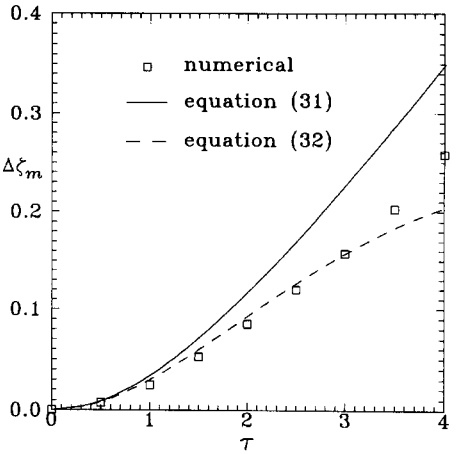

Fig. 6. Variation of the maximum point coordinate $\Delta\zeta_m$ with time τ. Points correspond to the numerical solution of equation (21), solid line represents the analytical solution (31), dashed line shows the solution (32).

differs from solution (31) only in the value of the factor in the second term. This solution presented in Fig. 6 by a dashed line fits the numerical results within the accuracy of 5%.

Thus, the numerical and analytical study presented in this paper shows that a thermal rising in an environment with altitude-dependent density has a quasi-shape-preserving structure. Density diminution with height causes some additional smearing of the top edge of the rising cloud and increase in the thermal radius. However, the main features of the self-similar thermal which are valid for an incompressible atmosphere-ascent law $z_t \sim t^{1/2}$ and the temperature decay as $t^{-3/2}$ still hold even as the ambient density at the level of the cloud top diminishes an order of magnitude compared to the density at the level where the initial heat release occurred.

Acknowledgements—The authors would like to thank the Royal Society and the EPSRC (grant GR/K 13486) for support of this study.

REFERENCES

1. J. Turner, *Buoyancy Effects in Fluids*. Cambridge University Press, Cambridge (1973).
2. Y. Jaluria, *Natural Convection Heat and Mass Transfer*. Pergamon Press, Oxford (1980).
3. A. T. Onufriev, Theory of the motion of vortex ring under the influence of gravity. Ascent of the atomic blast cloud, *Prikl. Mekh. Tekhn. Fiz.* **1**, 3–15 (1967).
4. B. R. Morton, Weak thermal vortex rings, *J. Fluid Mech.* **9**, 107–118 (1960).
5. G. T. Csanady, The buoyant motion within a hot gas plume in a horizontal wind, *J. Fluid Mech.* **22**, 225–239 (1965).
6. A. A. Berezovskii and F. B. Kaplanskii, Buoyant vortex ring in a viscous fluid, *Izv. Akad. Nauk SSSR, Mekh. Zhidk. Gaza* **3**, 42–48 (1989).
7. V. M. Mal'bakhov, On the theory of thermals in quiescent atmosphere, *Izv. Akad. Nauk SSSR, Fiz. Atm. Okeana* **8**, 683–694 (1972).
8. Yu. A. Gostintsev, A. F. Solodovnik and V. V. Lazarev, On the theory of aerodynamics, self-ignition and com-

bustion of turbulent thermals, vortex rings and plumes in open atmosphere, *Khim. Fizika* **9,** 1279–1290 (1982).
9. Yu. A. Gostintsev, V. V. Lazarev, A. F. Solodovnik and Yu. V. Shatskikh, Turbulent thermal in stratified atmosphere, *Izv. Akad. Nauk SSSR, Mekh. Zhidk. Gaza* **6,** 141–153 (1986).
10. D. Fox, Numerical simulation of the three-dimensional, shape-preserving convective element, *J. Atmos. Sci.* **29,** 322–341 (1972).
11. F. B. Kaplanskii and A. M. Epstein, Numerical study of free convection from a sudden heat release in a viscous liquid, *Inzh.-Fiz. Zhurnal* **33,** 700–704 (1977).
12. Yu. A. Gostintsev, Yu. S. Matveev, V. E. Nebogatov and A. F. Solodovnik, Turbulent thermal in stratified atmosphere, *Prikl. Mekh. Tekhn. Fiz.* **6,** 141–153 (1986).
13. G. M. Makhviladze, O. I. Melikhov and S. E. Yakush, On the numerical simulation of the ascent of a turbulent thermal in a non-uniform compressible atmosphere, *Izv. Akad. Nauk SSSR, Mekh. Zhidk. Gaza* **1,** 72–80 (1989).
14. G. M. Makhviladze, O. I. Melikhov and S. E. Yakush, Ascent of a turbulent axisymmetric thermal in a non-uniform compressible atmosphere, *Prikl. Mekh. Tekhn. Fiz.* **1,** 62–68 (1989).
15. G. M. Makhviladze and S. E. Yakush, Self-similar axisymmetric thermal in a medium with non-uniform density distribution, *Izv. Akad. Nauk SSSR, Mekh. Zhidk. Gaza* **4,** 45–53 (1991).
16. D. P. Bacon and R. A. Sarma, Agglomeration of dust in convective clouds initialized by nuclear bursts, *Atmos. Environ.* **25A,** 2627–2642 (1990).
17. W. M. Kays, Turbulent Prandtl number—where are we? *Trans. ASME J. Heat Transfer* **116,** 284–295 (1994).
18. Yu. A. Gostintsev and A. F. Solodovnik, Powerful turbulent thermal in a stably stratified atmosphere, *Prikl. Mekh. Tekhn. Fiz* **1,** 47–53 (1987).
19. D. Anderson, R. H. Pletcher and J. C. Tannehill, *Computational Fluid Mechanics and Heat Transfer.* Hemisphere, New York (1984).
20. M. Abramowitz and I. A. Stegun, *Handbook of Mathematical Functions.* Dover, New York (1970).
21. I. S. Gradshteyn and I. M. Ryzhik, *Table of Integrals, Series and Products* (4th Edn), p. 950. Academic Press, New York (1965).